



Towards a refined model for predicting geoneutrino signal at SNO+

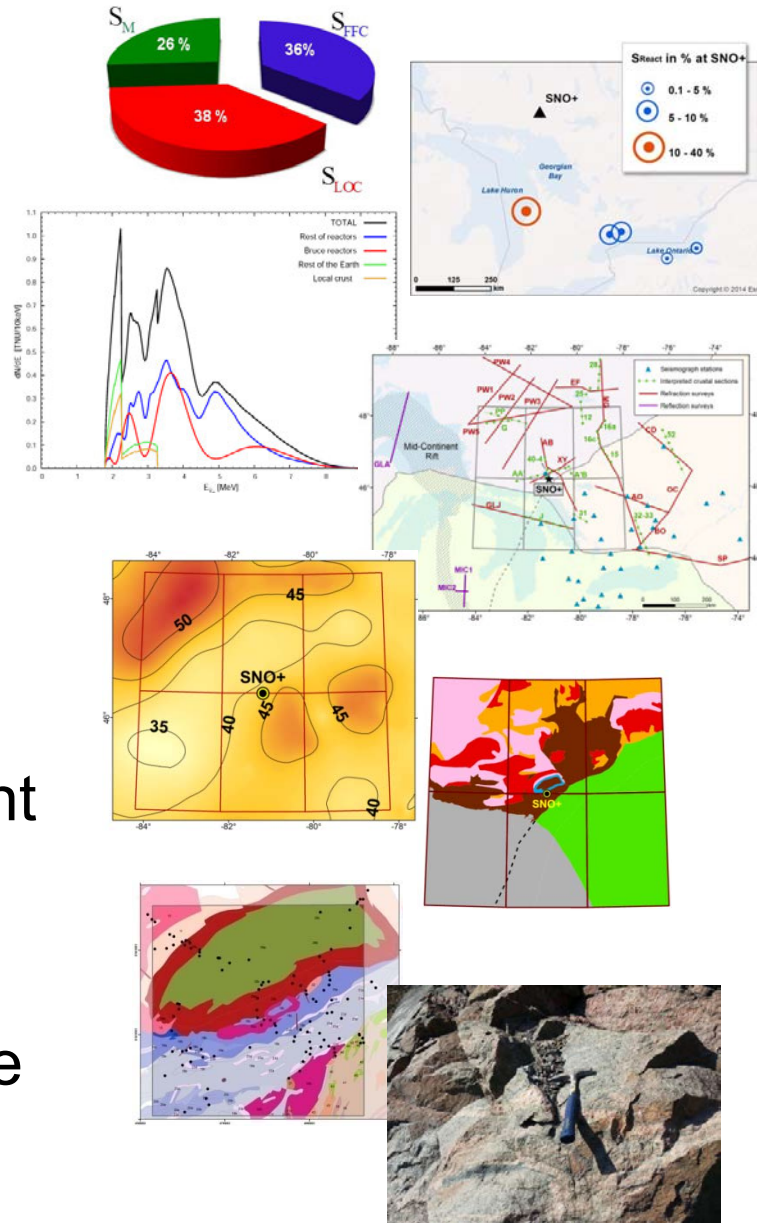
Virginia Strati PhD
University of Ferrara & INFN
strati@fe.infn.it

Scott A. Wipperfurth - William F. McDonough (University of Maryland)
Marica Baldoncini – Fabio Mantovani (University Ferrara - INFN)

International Workshop
“Neutrino Research and Thermal Evolution of the Earth”
Sendai, 26 March 2016

Outline

- Contributions to geoneutrino and reactor antineutrino signal at SNO+
- Modeling the geoneutrino flux
- The 3D model of the crust surrounding SNOLAB
- Geoneutrino signals from the different crustal reservoirs
- The next steps: focusing on the close crust



Detecting geoneutrino signals around the world

In one site, for each radioisotope (^{238}U , ^{232}Th) the expected geoneutrino signal is the sum of three contributions:

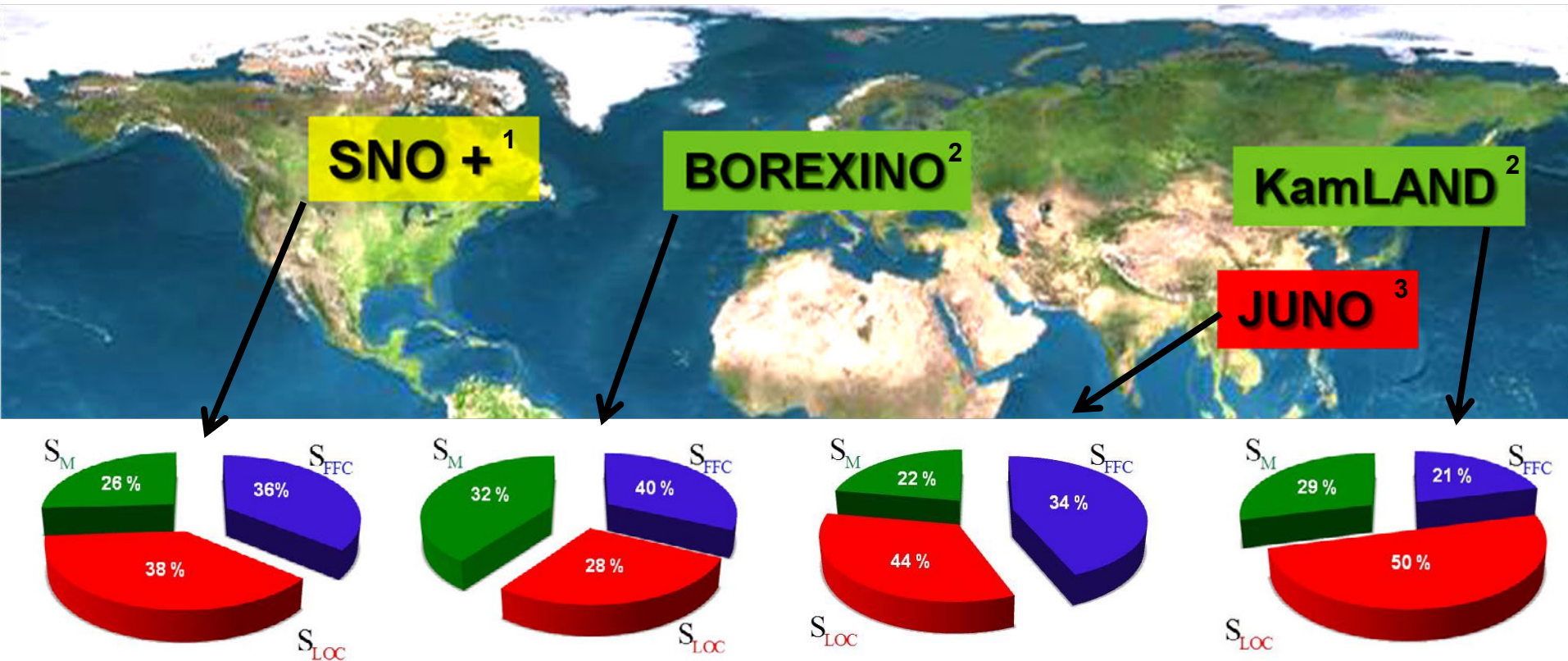
$$S_{\text{EXP}} = S_{\text{LOC}} + S_{\text{FFC}} + S_{\text{M}}$$

EXP = total expected signal

LOC = crust of the region within some hundreds km from the detector

FFC = Far Field Crust

M = mantle signal

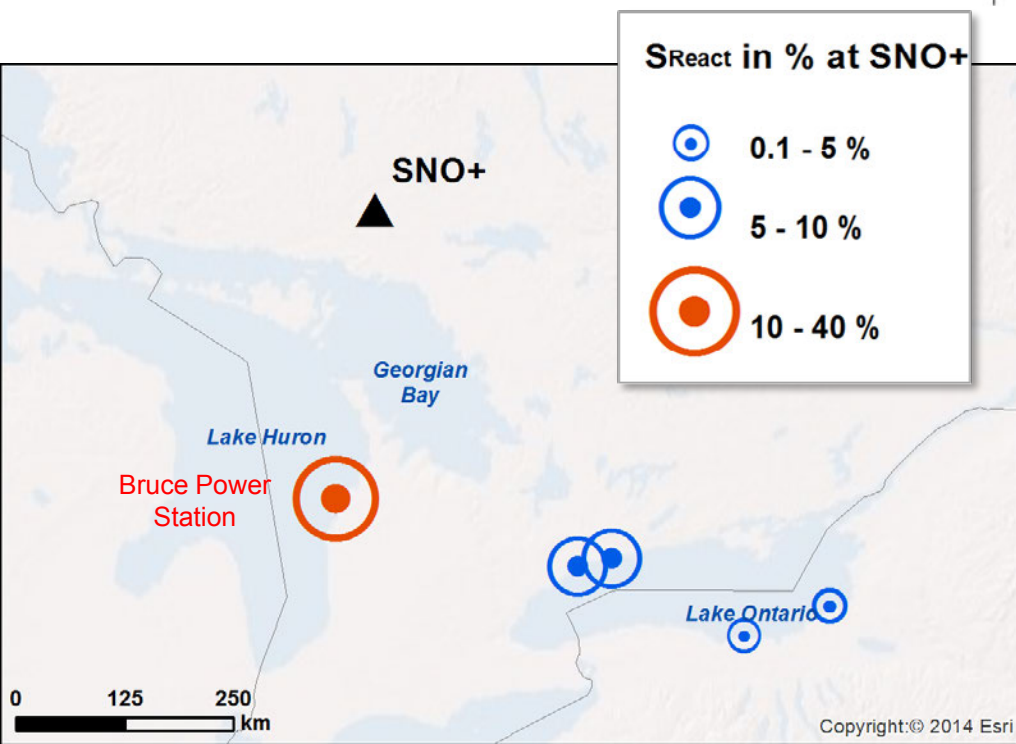
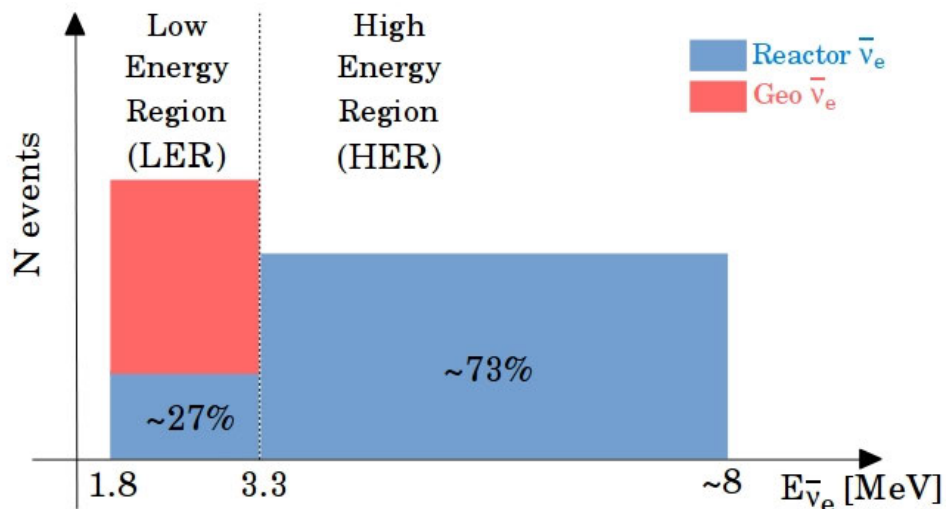


1 – Huang et al. 2014, Geochemistry, Geophysics, Geosystems.

2 - Fiorentini et al 2012, Physical Review D. 3 - Strati et al. 2015, Progress in Earth and Planetary Science.

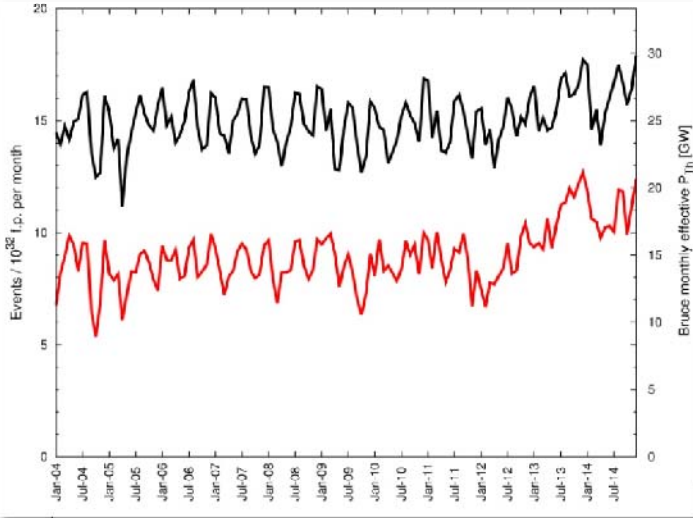
Reactor antineutrinos signal at SNO+

- Reactor antineutrinos are the most severe background for geoneutrino measurements.
- In the **Low Energy Region (LER)** we observe an overlap between geoneutrino and reactor antineutrinos spectra, with a signal ratio $S_{\text{LER}}/S_{\text{Geo}} \sim 1$ at SNO+

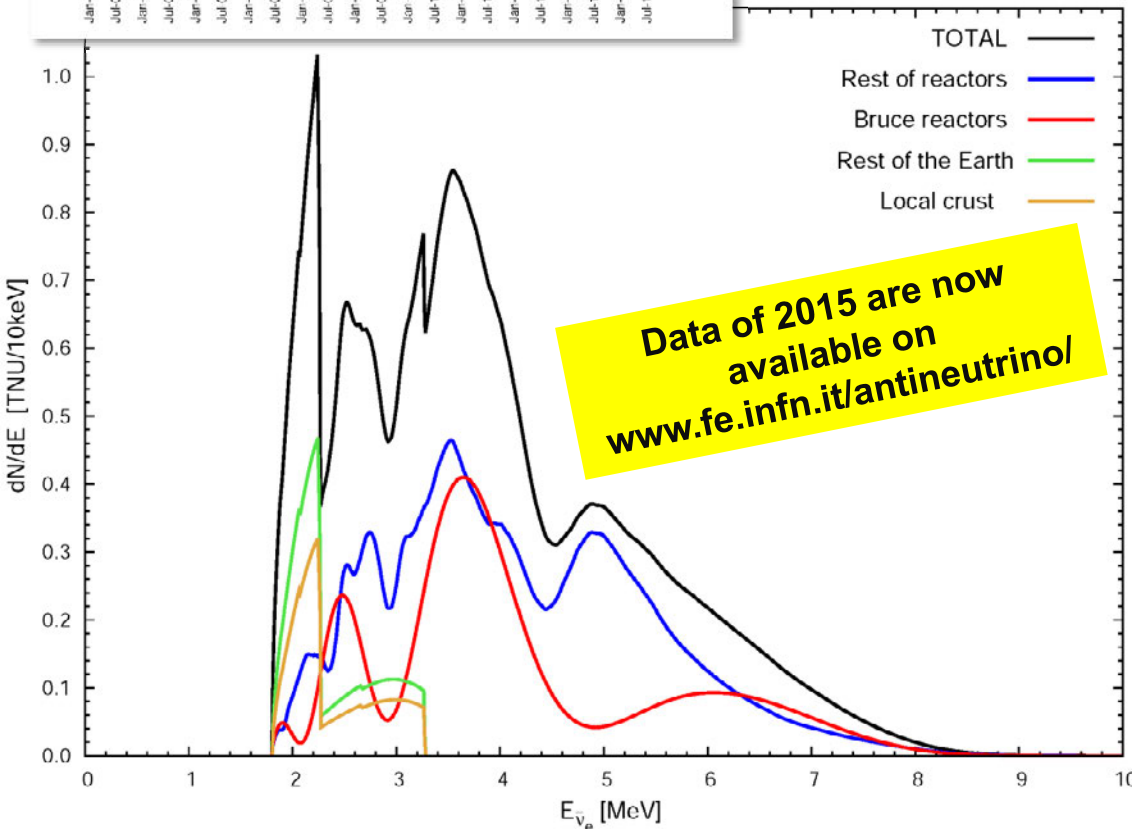


- **Bruce Power Station** includes 8 nuclear reactors and produces **~22 GW** of thermal power.
- Although the thermal power of Bruce reactors corresponds to 1.9% of the global thermal power, they contribute to about **38%** of total reactor antineutrino signal S_{React} at SNO+.

Reactor antineutrinos and geoneutrino at SNO+



- The temporal fluctuations ($\sim 10\%$ at 1σ) of **reactor antineutrino signal** resembles the temporal profile of the **Bruce Power Station** effective thermal power.
- The geoneutrino signal of the **Local Crust** corresponds to $\sim 50\%$ of the total crustal signal.



Geoneutrinos signal¹(TNU)

Local Crust	15.6^{+5.3}_{-3.4}
Rest of the Crust	15.1 ^{+2.8} _{-2.4}
Cont. Lithos. mantle	2.1 ^{+2.9} _{-1.2}
Mantle	9
TOTAL	40 ⁺⁶ ₋₄

Reactor antineutrinos signal² (TNU)

	LER	FER
Bruce reactors	17.3 ^{+1.0} _{-0.7}	73.7 ^{+2.0} _{-1.8}
Rest of reactors	31.2 ^{+0.9} _{-0.8}	118.9 ^{+2.8} _{-2.6}
TOTAL	48.5 ^{+1.8} _{-1.5}	192.6 ^{+4.7} _{-4.4}

1 - Huang et al. 2014 Geoch. Geoph. Geosys.

2 - Baldoncini et al. 2016 Journal of Physics: Conference Series.

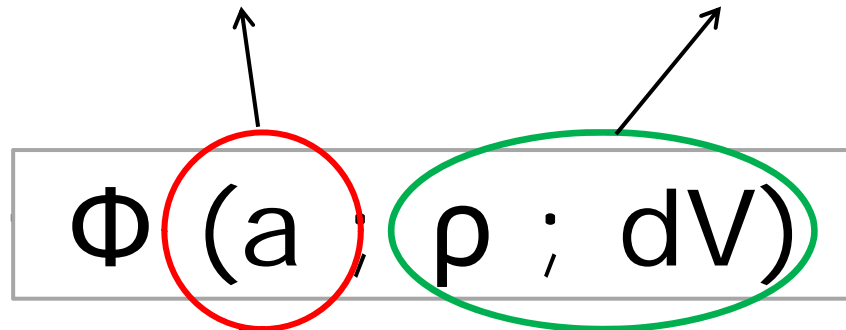
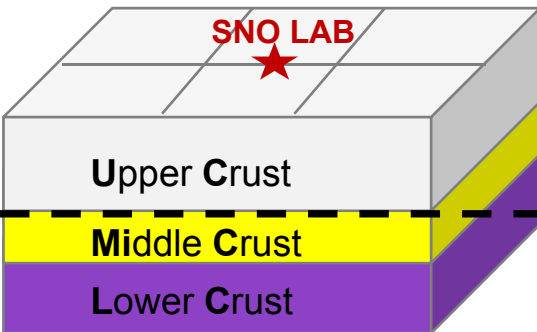
Modeling the geoneutrino flux

$$\phi(\mathbf{X}) = \frac{\epsilon_{\bar{\nu}_X}}{4\pi} \int_V \frac{\rho(\vec{r}') a_X(\vec{r}')}{|\vec{R} - \vec{r}'|^2} dV'$$

UC

U and Th abundances from published database

Literature data, geological maps and interpreted seismic profiles



MC

U and Th abundances inferred from seismic arguments

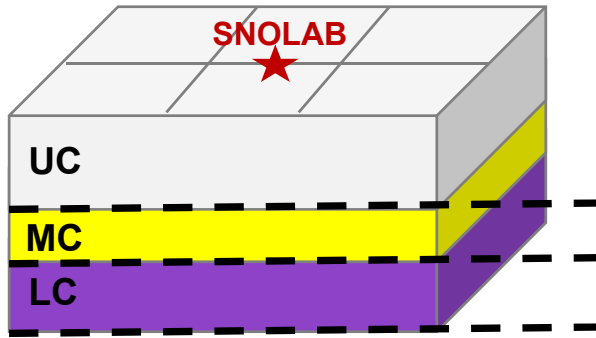
Estimations from seismic velocities

LC

Geochemical uncertainties
~ 15%

Geophysical uncertainties
~ 5%

The 3D geophysical model



?

- The first step of the construction of the 3D model is defining the local crustal structure and **Moho Discontinuity** depth.
- The boundaries between **Upper, Middle** and **Lower Crust** will be identified on the base of seismic velocities.

The necessary geophysical inputs come mainly from seismic experiments:

ACTIVE METHODS

$\delta v \sim 2\%$

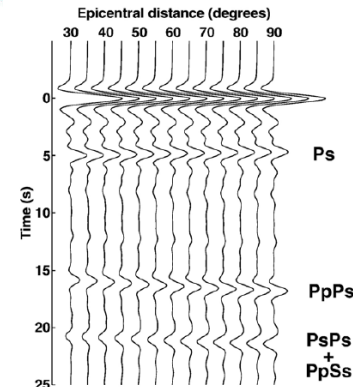
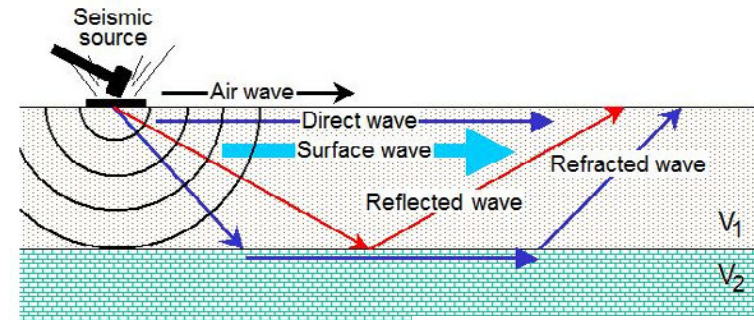
2D Velocity Models

- Refraction surveys
- Reflection surveys

PASSIVE METHOD

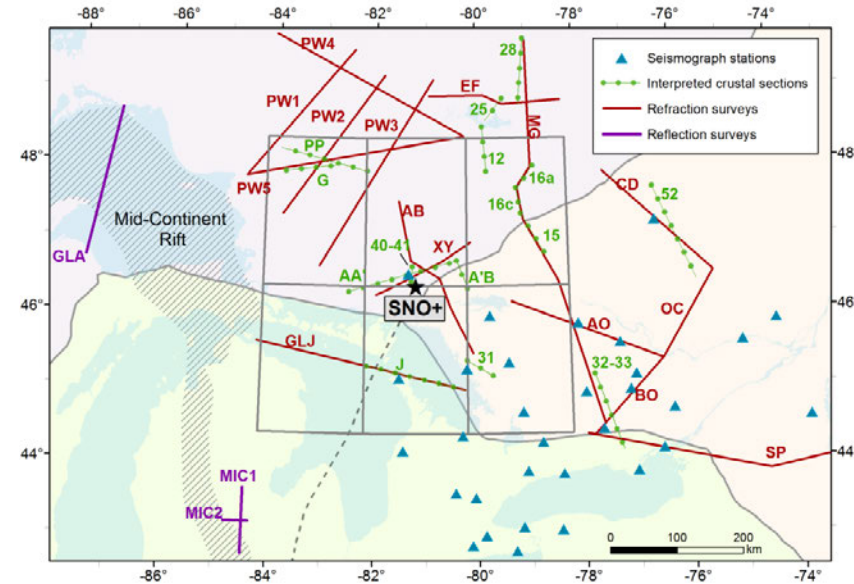
$\delta H \sim 1\%$

- **Teleseismic data:** the crustal thickness is inferred through the analysis of data from distant earthquakes acquired by a network of seismic stations.



The 3D model of the crust surrounding SNO+

- The refined 3D model of the local crust is built using **refraction** seismic data collected in the last 30 years.
- **Reflection seismic** surveys and teleseismic acquisitions provide additional constraints on the crustal thickness.



Huang et al. 2014, Geochemistry, Geophysics, Geosystems

Experiment	Main investigated areas	N° of lines	Type	Reference
LITHOPROBE	Sudbury Basin	2	Refraction	Winardhi and Mereu (1997)
	Superior Province	2	Refraction	Winardhi and Mereu (1997)
	Kapuskasing Structural Zone	5	Refraction	Percival and West (1994)
COCRUST	Grenville Province	4	Refraction	Mereu et al. (1986)
O-NYNEX	Appalachian Province	1	Refraction	Musacchio et al. (1997)
GLIMPCE	Great Lakes	1	Refraction	Epili and Mereu (1991)
		1	Reflection	Spence et al. (2010)
COCORP	Michigan Basin	2	Reflection	Brown et al. (1982)

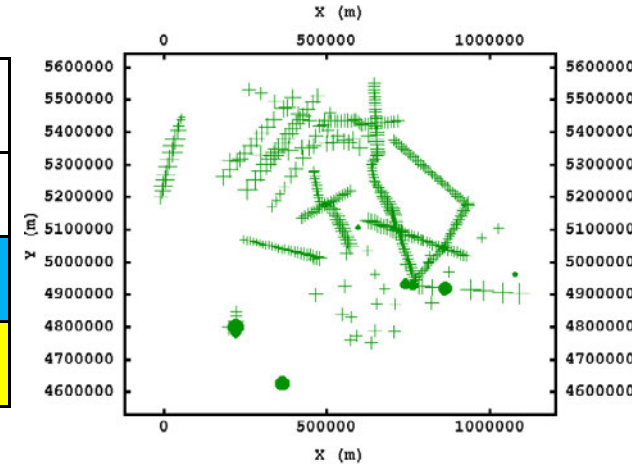
Modeling the TMC, TLC and MD

Inputs

Depth-controlling points obtained by 15 refraction lines, 3 reflection lines and data from 32 seismographic stations.



	N° points
Top of MC (TMC)	343
Top of LC (TLC)	343
Moho discontinuity (MD)	392

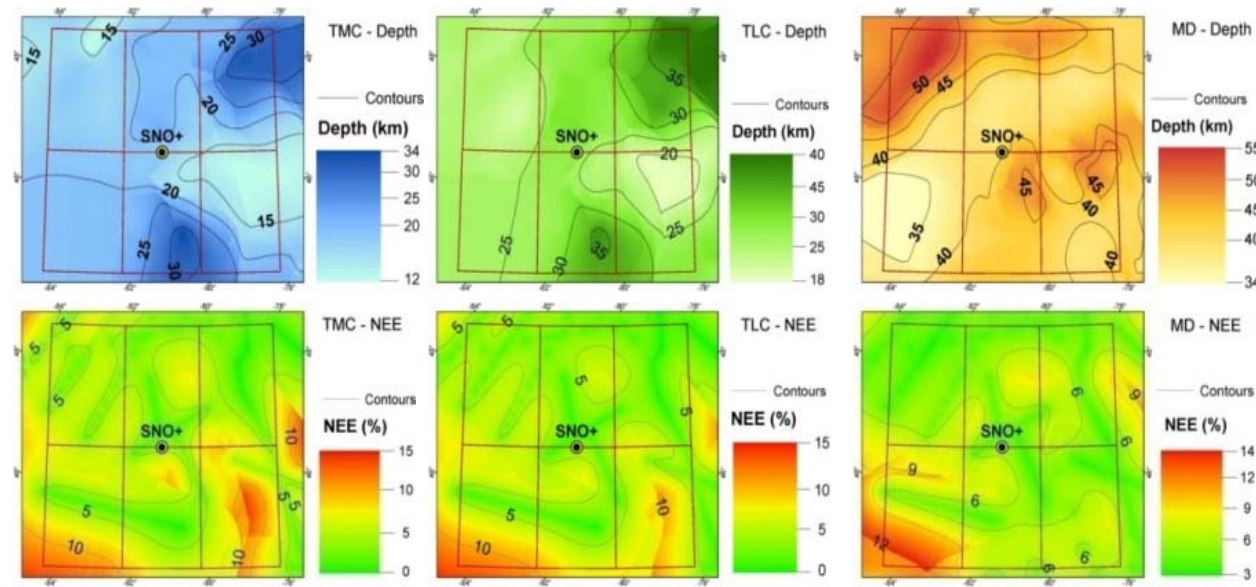


ORDINARY KRIGING: a stochastic estimator that considers the **spatial continuity** of input variables and infers the values in unobserved locations providing the result in term of **probability**: it's possible to quantify the **estimation errors**.

Output



- Estimated maps of TMC, TLC and MD depth with a 1 km × 1 km resolution.
- Maps provides the Normalized Estimation Errors (NEE).



The Ordinary Kriging method

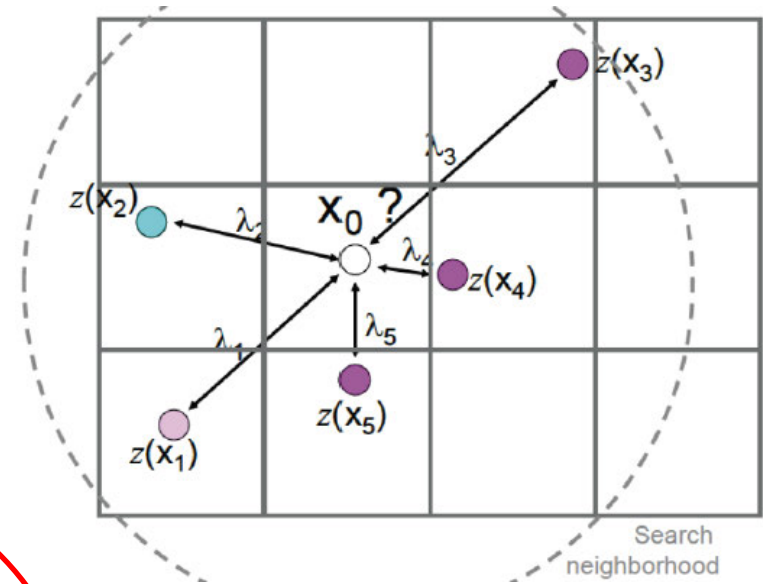
GENERAL ESTIMATOR

$$z^*(x_0) = \sum_{i=1}^n \lambda_i z(x_i)$$

x_0 = target point

$z(x_i)$ = measured samples

λ_i = weight assigned to the samples



Different weights on the base of the spatial correlation

Goals:

- Minimization of the variance of the estimate (kriging variance)
- Distribution of the predictions similar to the distribution of the real values.

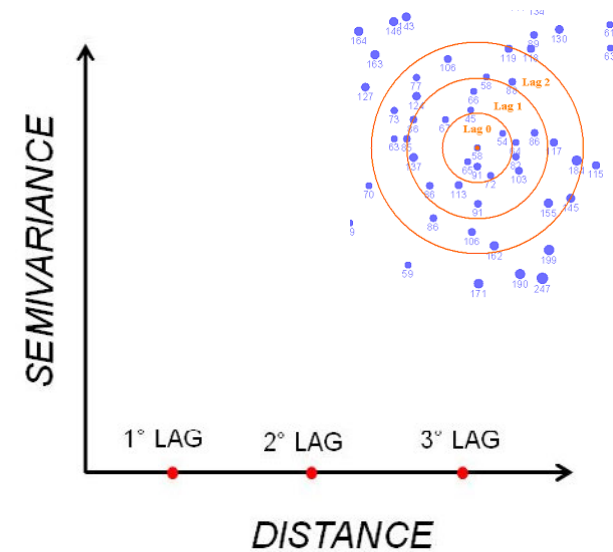
Spatial variability of the crustal discontinuity in Sudbury region

Experimental Semi-Variogram (ESV):

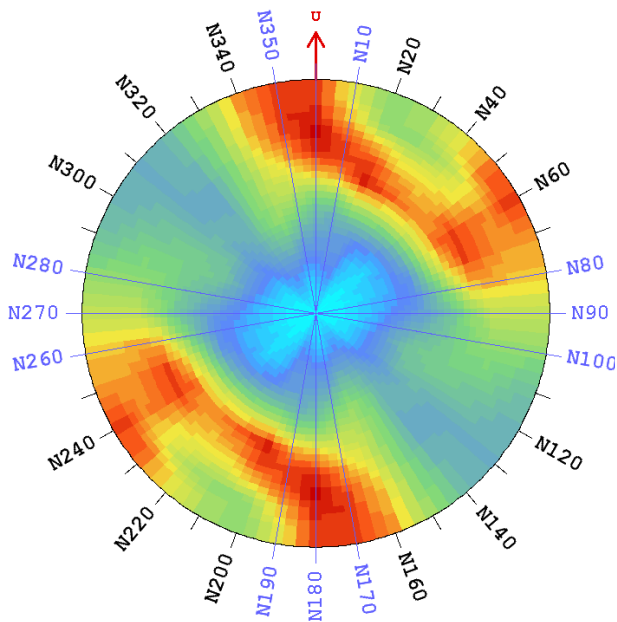
$$\gamma(h) = \frac{1}{2m(h)} \sum_{i=1}^{m(h)} [Z(x_i + h) - Z(x_i)]^2$$

$m(h)$ = number of sample value pairs within distance h

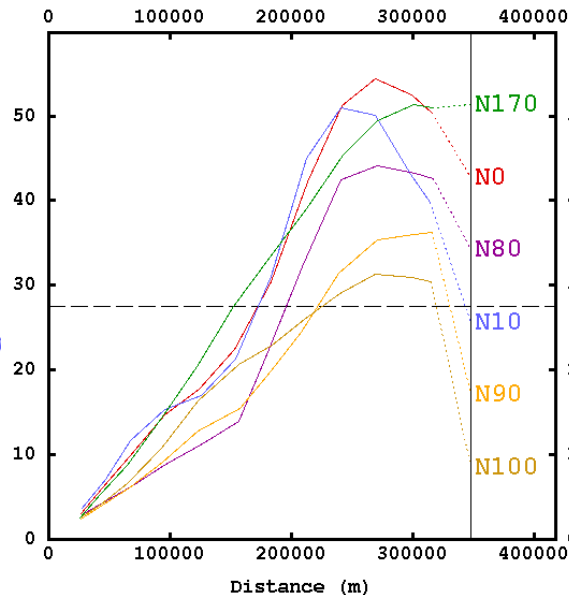
The **number** and the **dimensions** of the lags depend on features of the dataset and spatial distribution of the samples.



Variogram Map



Top of the Lower Crust



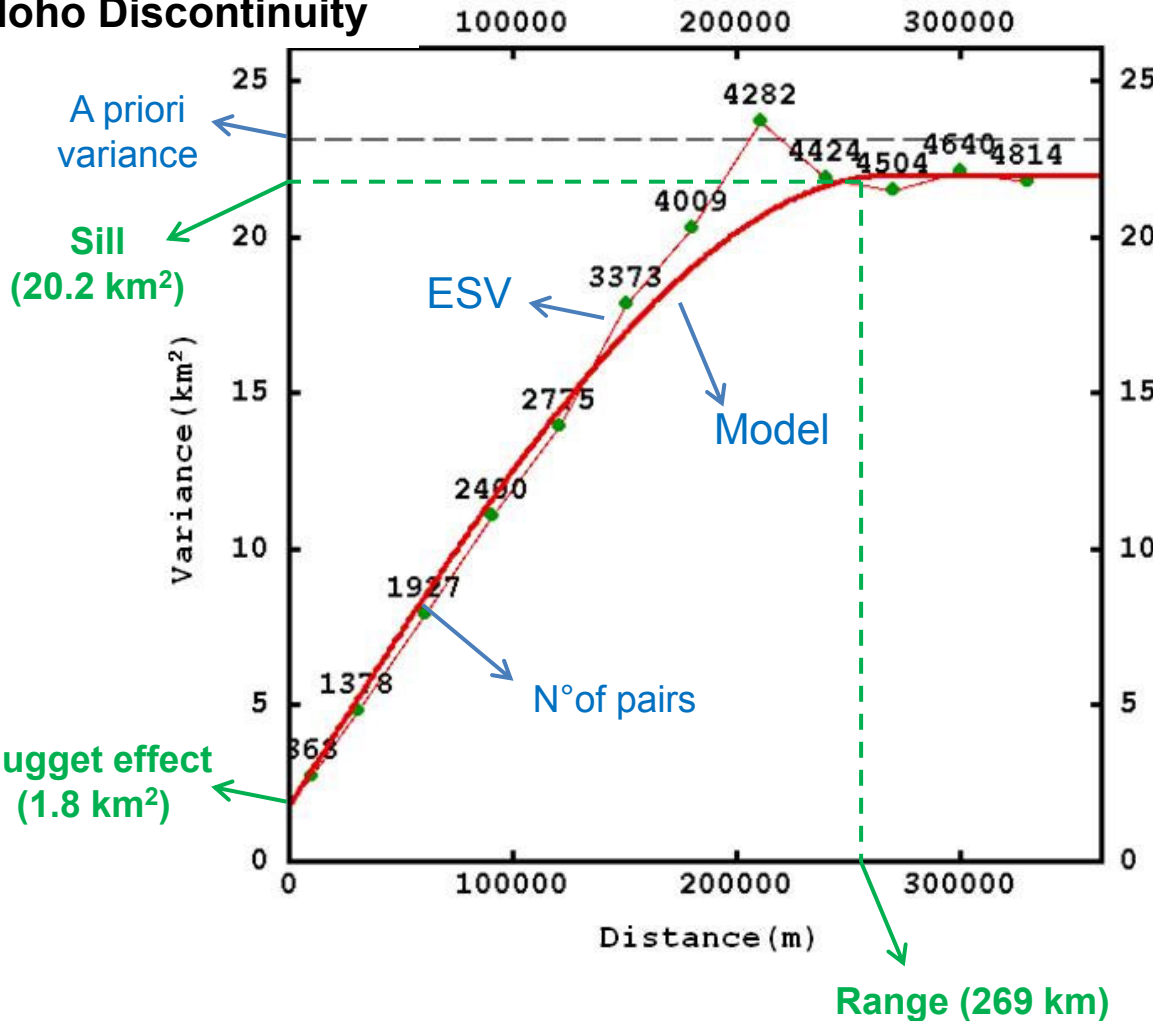
The semivariogram is computed for **different directions** in the space: in the first lags there aren't preferred directions of variability.

For each surface, an **omnidirectional ESV** with **12 lags** of **30 km** is computed.

The semivariogram modeling

- A theoretical function (e.g. spherical, exponential, gaussian) is used to describe the experimental semivariogram.
- The **model parameters** are tested and the best fit is chosen.

Moho Discontinuity



1) NUGGET EFFECT

$\gamma(0) \sim 5\%$ of the total spatial variability

There is a good correlation between adjacent points from different seismic lines.

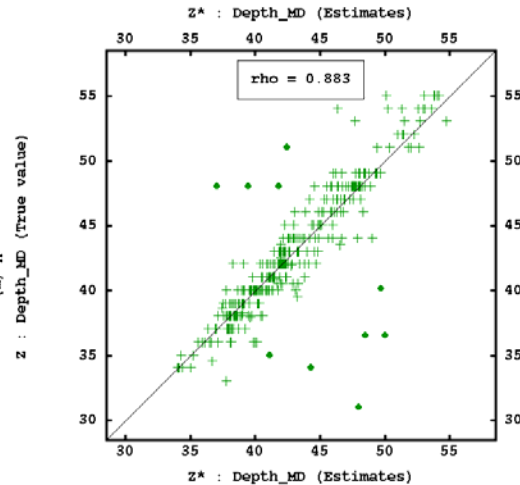
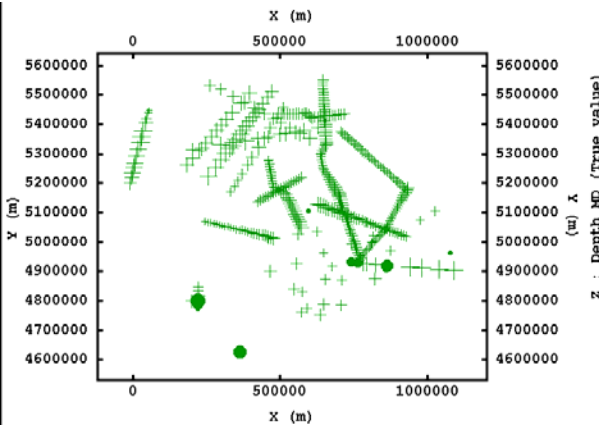
2) SPHERICAL STRUCTURE

For $h > \text{'Range'}$ the data are not spatial correlated and the γ is constant and corresponds to **'Sill'**.

The Cross Validation

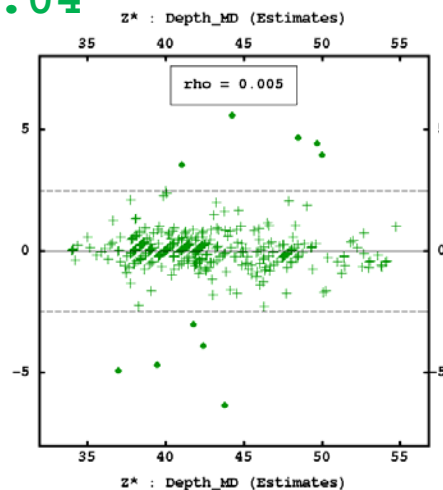
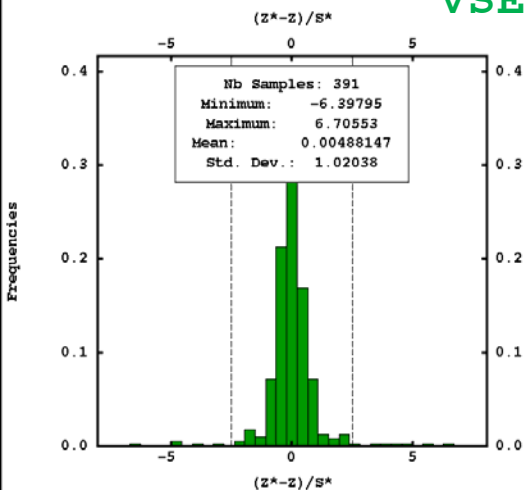
This procedure allows for testing different models and for verifying the compatibility between the dataset and the structural model.

Moho Discontinuity



MSE = 0.005

VSE = 1.04



- Each sample is in turn assumed as a missing value and the estimates are realized.
- For each sample we have the **real value** and the **estimated value**.



Mean Standardized Errors $\rightarrow 0$

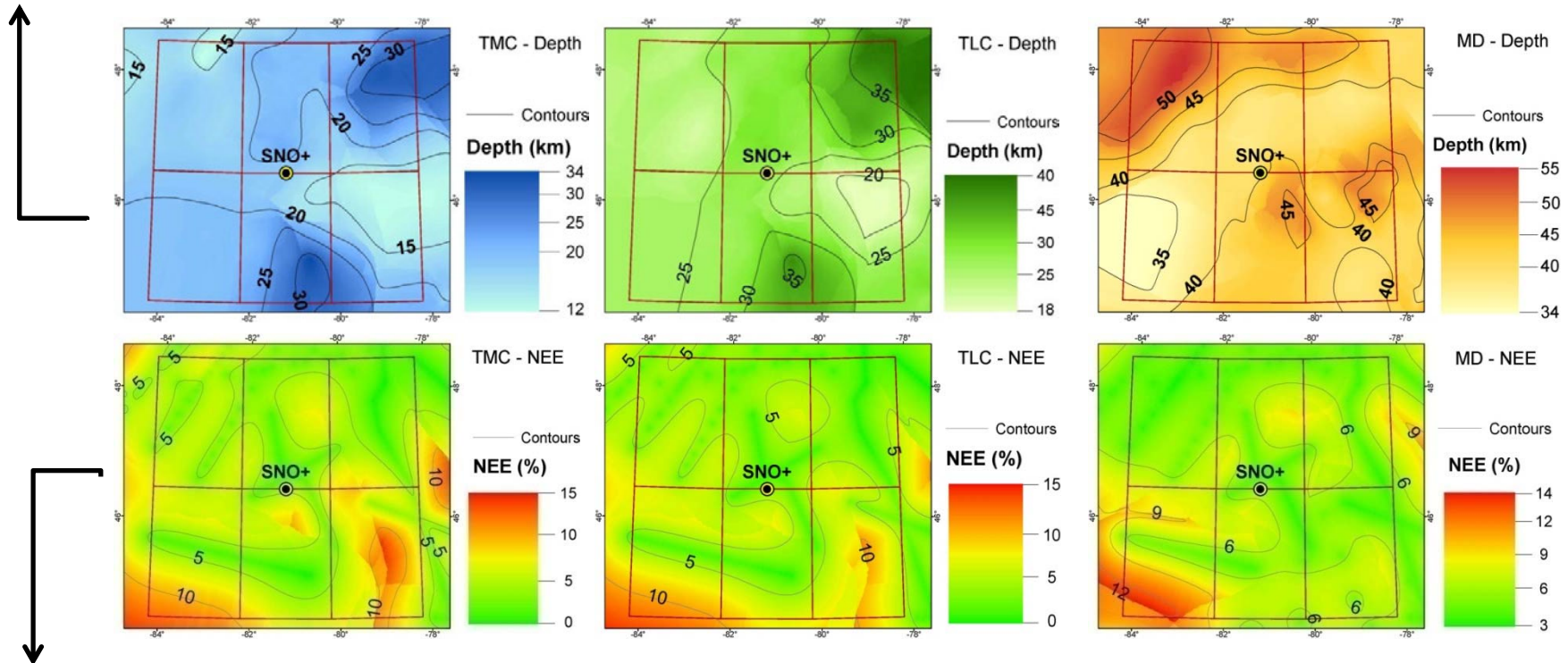
$$MSE = \frac{1}{N} \sum_{i=1}^N \frac{\{z^*(x_i) - z(x_i)\}}{\sigma(x_i)}$$

Variance Standardized Errors $\rightarrow 1$

$$VSE = \frac{1}{N} \sum_{i=1}^N \frac{\{z^*(x_i) - z(x_i)\}^2}{\sigma^2(x_i)}$$

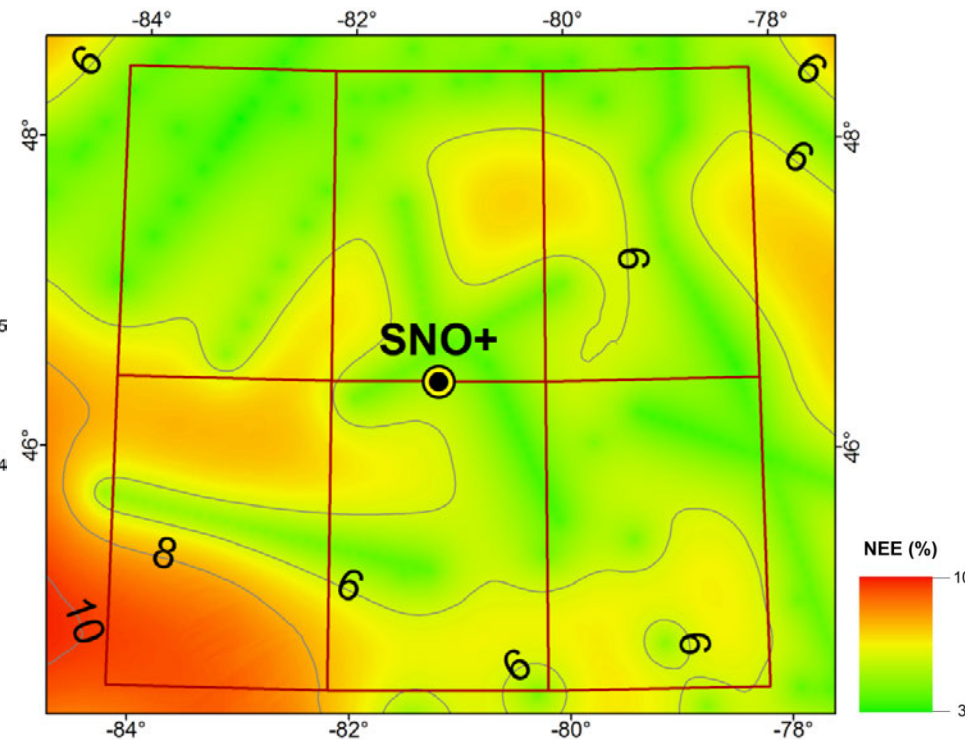
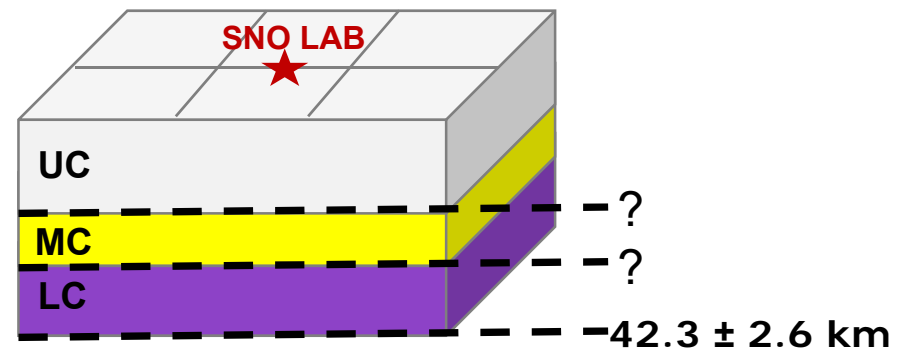
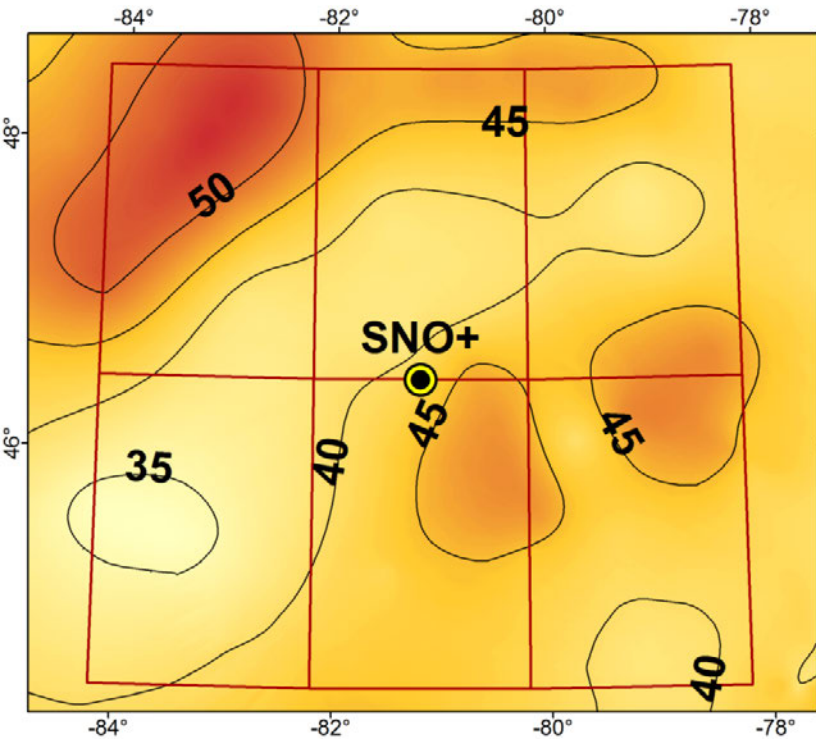
The results of the spatial interpolation

Map of the crustal depths: the continuous models of the three surfaces have been obtained in the form of a regular GRID file. The estimations in each 1 km x 1 km cell are performed on the base of the study of spatial correlation.



Normalized Estimation Errors (NEE) maps: the uncertainties of the estimation in terms of variance are obtained and are normalized with respect to the estimated values of the depth. They are expressed in the maps in percentage.

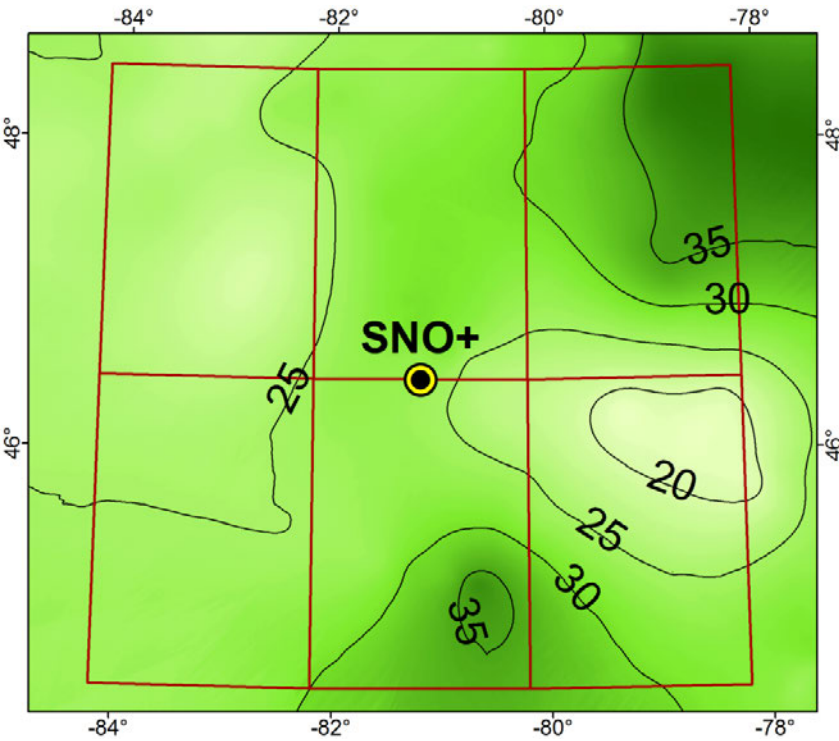
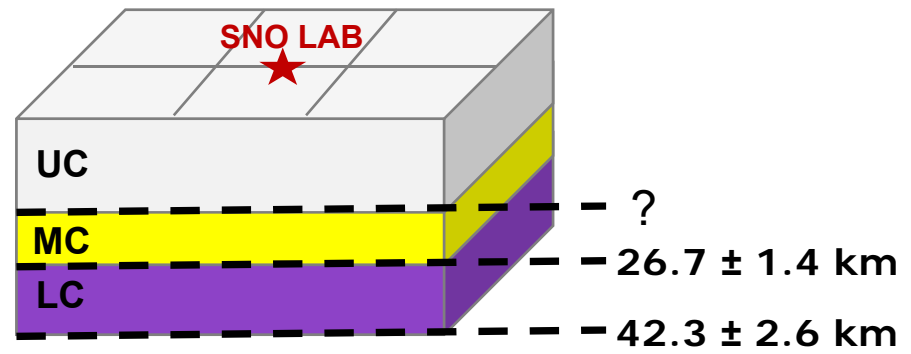
Moho Discontinuity



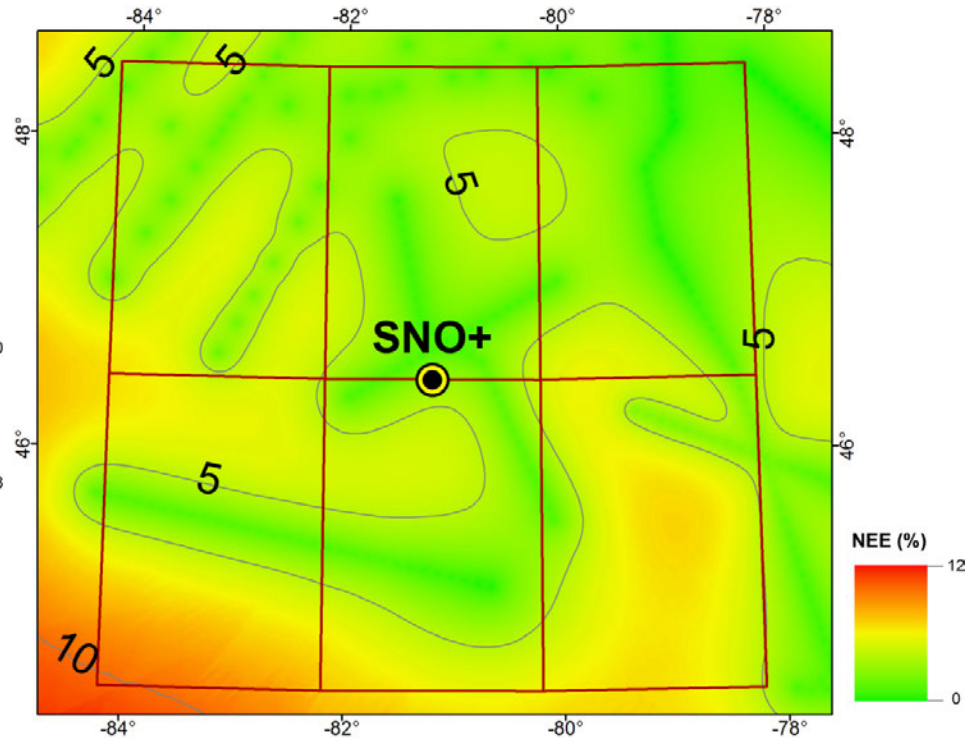
The depth map of the MD highlights the presence of the **Grenville Front Tectonic Zone** and the **Kapuskasing Structural Zone**.

In the velocity models, the Moho discontinuity is marked by an evident increase of the P-wave velocity. It constrains the average crustal thickness at **6%** level.

Top of the Lower Crust

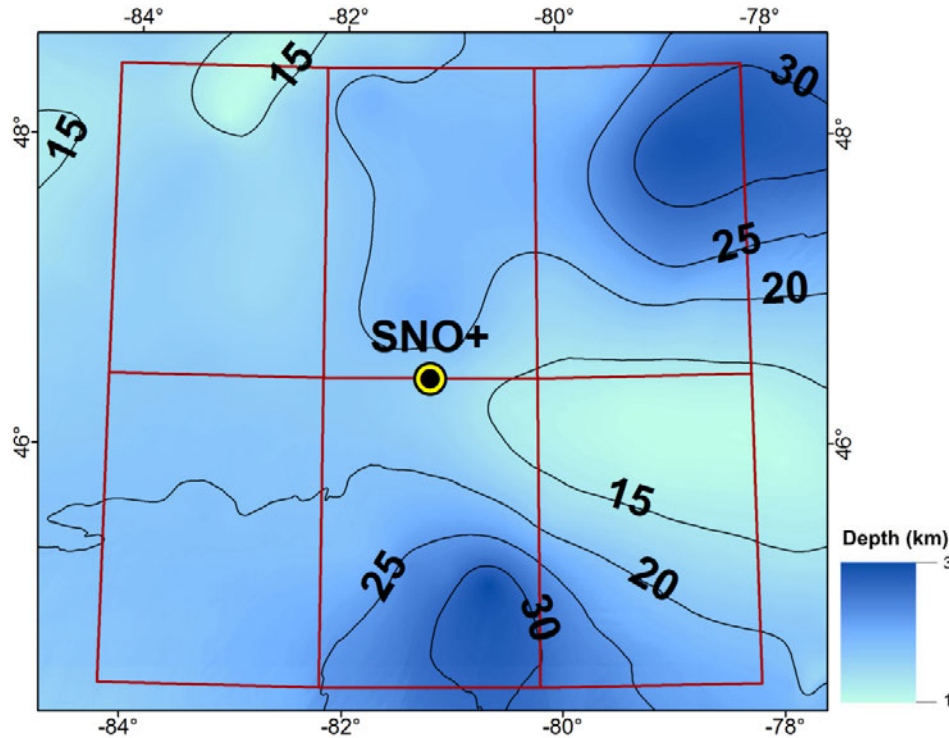


The depth of the TLC depth is rather constant in the **Superior Province** (about 25 km). In the **Grenville Province** is variable in a range comprised between 18 and 40 km.

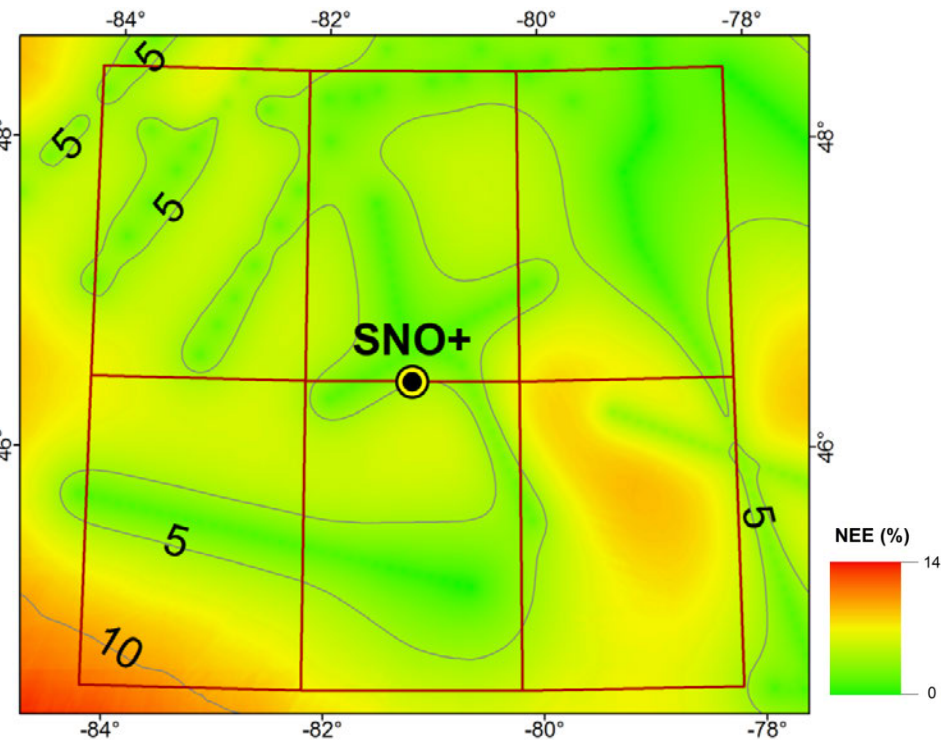
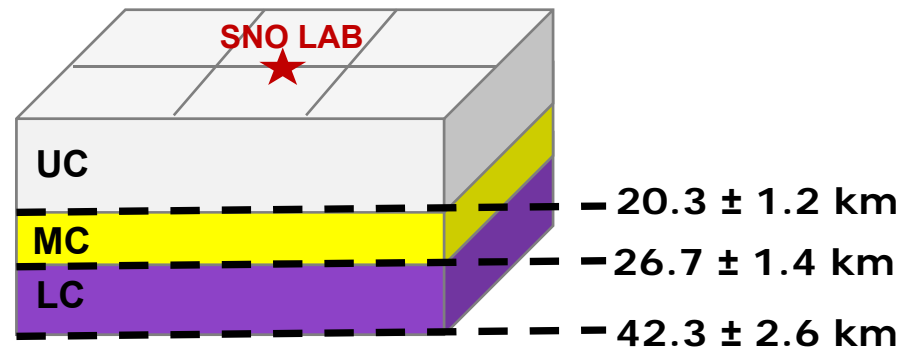


The values of the uncertainties are close to 1% in the sampled locations.

Top of the Middle Crust



According to the model, the **Upper Crust** accounts for about half of the thickness of the bulk regional crust and reaches the higher thickness in the **Grenville Province**.



The higher values of the uncertainties are obtained in the southwest of the area far from the detector.

Summary of geophysical uncertainties

- The realization of the continuous models of depth for the three surfaces allows for the calculation of the **thicknesses** and **volumes** of UC, MC and LC.
- These results, together with densities, permitted to estimate the **masses** of the main crustal reservoirs together with their uncertainties.

	CRUST 1.0*	Huang et al. 2014			
	M [10^{18} kg]	Thickness	Volume [10^6 km 3]	ρ [g/cm 3]	M [10^{18} kg]
UC	6.6	20.3 ± 1.1	4.2 ± 0.2	2.73 ± 0.08	11.5 ± 0.6
MC	8.1	6.4 ± 0.4	1.3 ± 0.1	2.96 ± 0.03	3.8 ± 0.3
LC	8.0	15.6 ± 1.0	3.2 ± 0.2	3.08 ± 0.06	9.9 ± 0.6
Total	22.7	42.3 ± 2.6	8.7 ± 0.5	-	25.2 ± 1.6

- The relative uncertainties of the reservoirs masses are of **~ 6%**.
- Respect to CRUST 1.0 this crustal model of the region surrounding SNOLAB estimates **geophysical uncertainties** and it is more refined because includes **local input data**.

* Laske et al. [2013] at <http://igppweb.ucsd.edu/~gabi/rem.html>

Refining the Upper Crust

Input

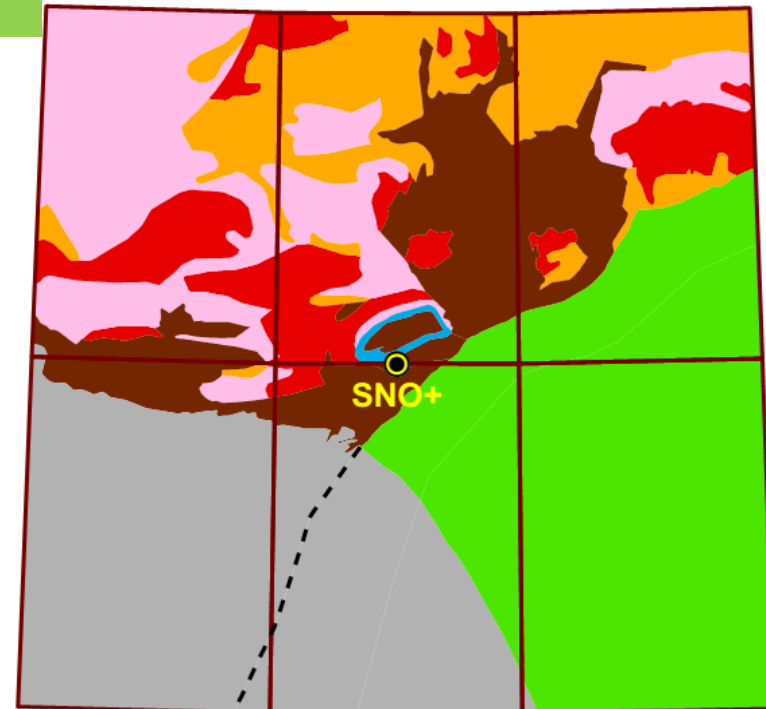
- Geological Map of North America - 1:500000 scale
- Geological cross sections
- Interpreted seismic profiles



7 lithologic units in the Upper Crust are clustered on the base of compositional, stratigraphic and evolutionary arguments.

-  Paleozoic sediments (Great Lakes)
-  Huronian Supergroup and Sudbury Basin rocks
-  Granite or granodioritic intrusions
-  Sudbury Igneous Complex
-  Volcanics and metavolcanics rocks
-  Tonalite and tonalite gneiss
-  Central Gneiss Belt

(Reed et al., 2005)

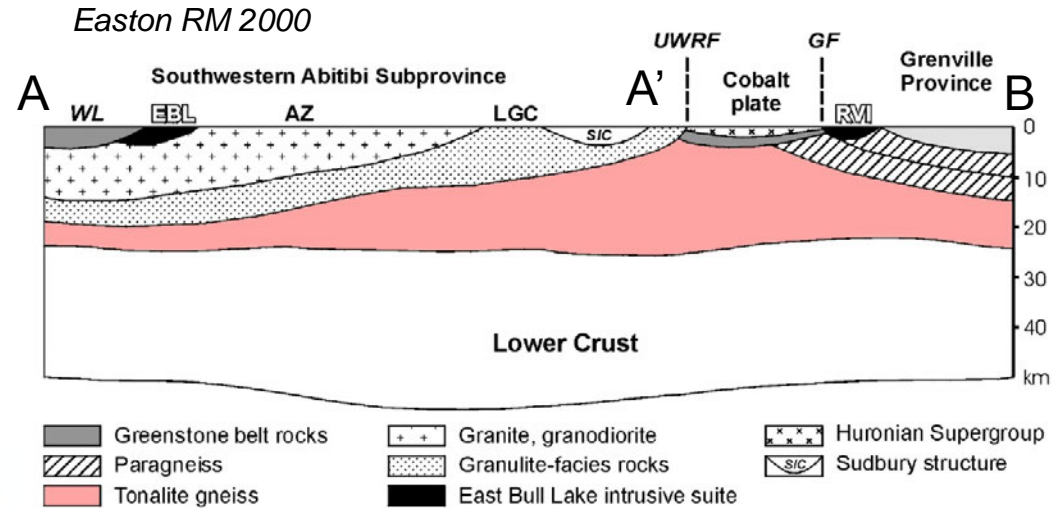
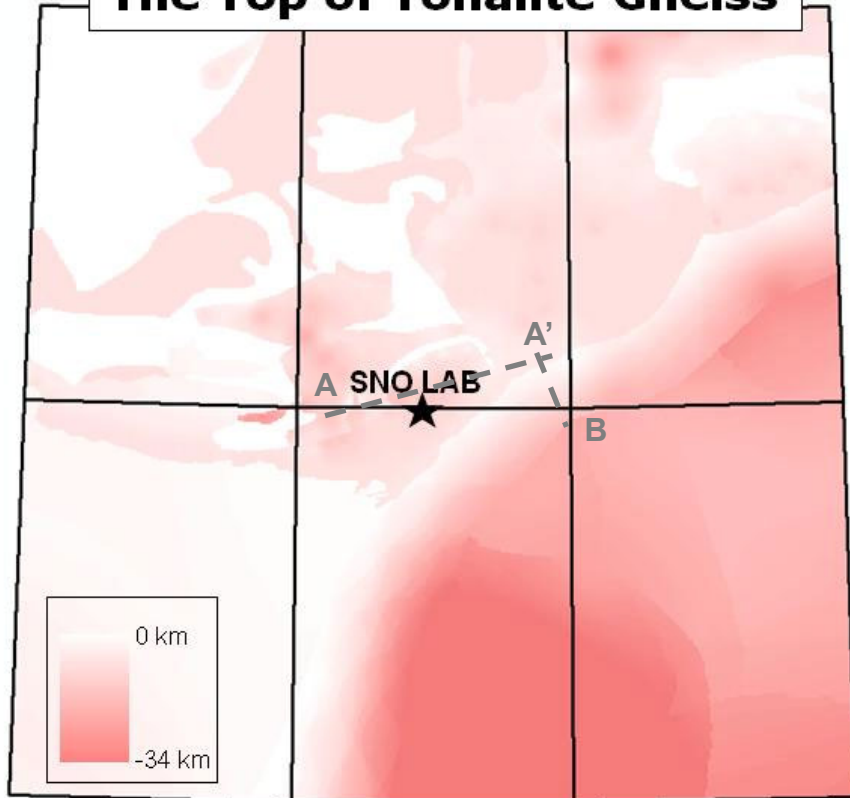


Modeling the 7 lithological units

Motivations

Although the volumes of these outcropping subreservoirs are often small, their U and Th content can vary of one order of magnitude.

The Top of Tonalite Gneiss

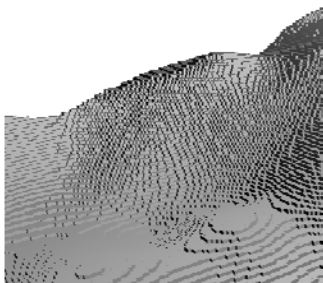


- The contacts between the 7 dominant lithological units in the physical model of upper crust are defined using 16 **interpreted crustal cross sections** of the area.
- For each lithologic unit the **top** and the **bottom** surfaces are obtained by spatial interpolation.

The numerical 3D Model

Input

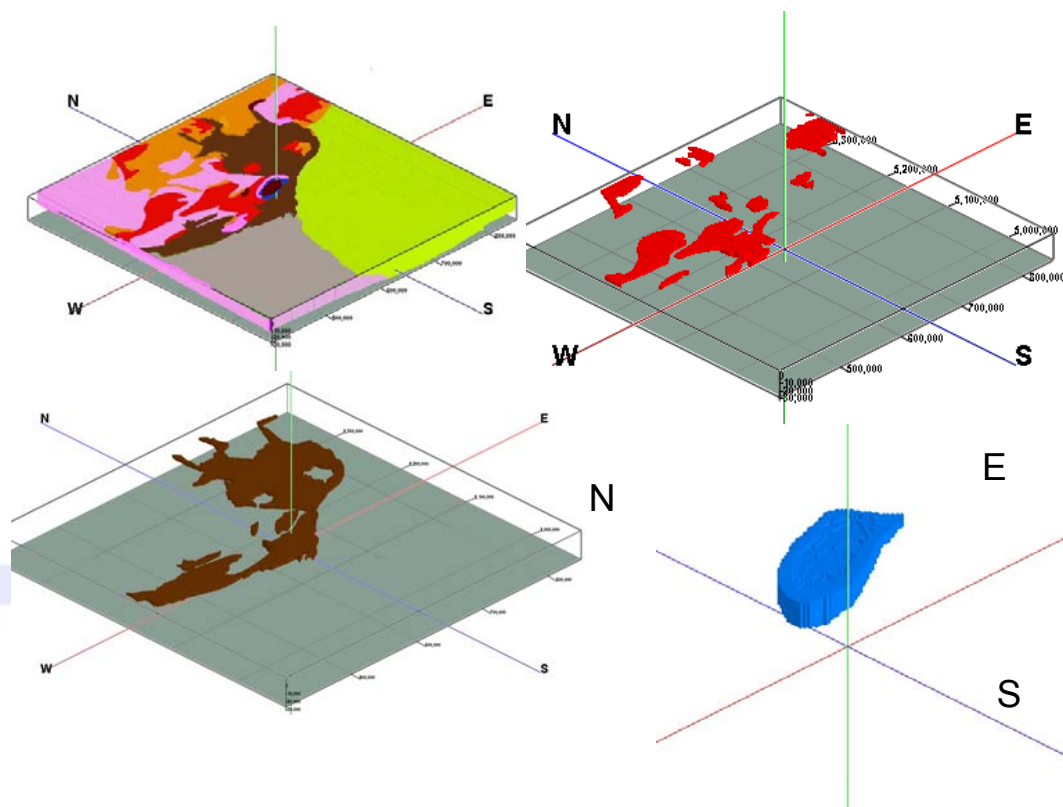
GRIDS of surfaces of MD, TLC, TMC and the top and the bottom of each lithological unit.



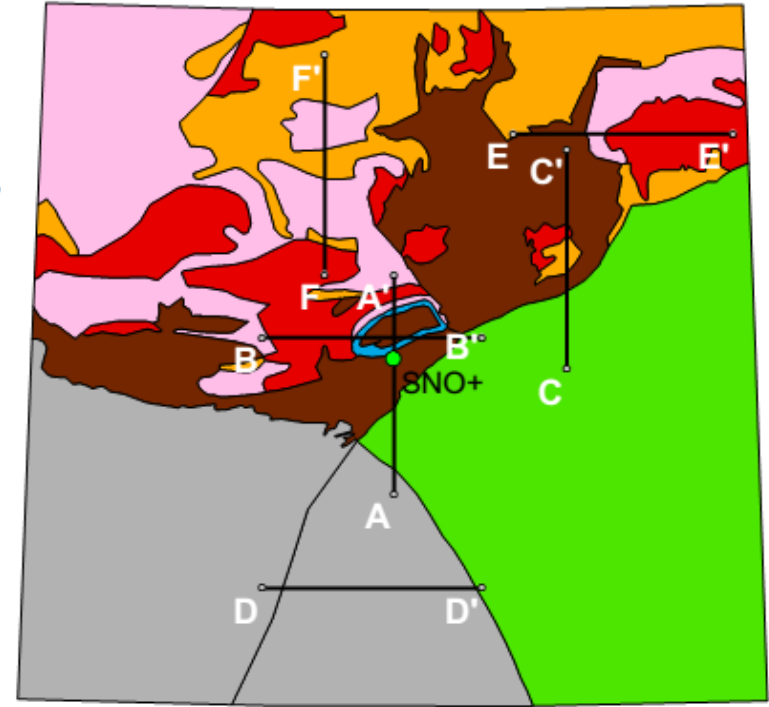
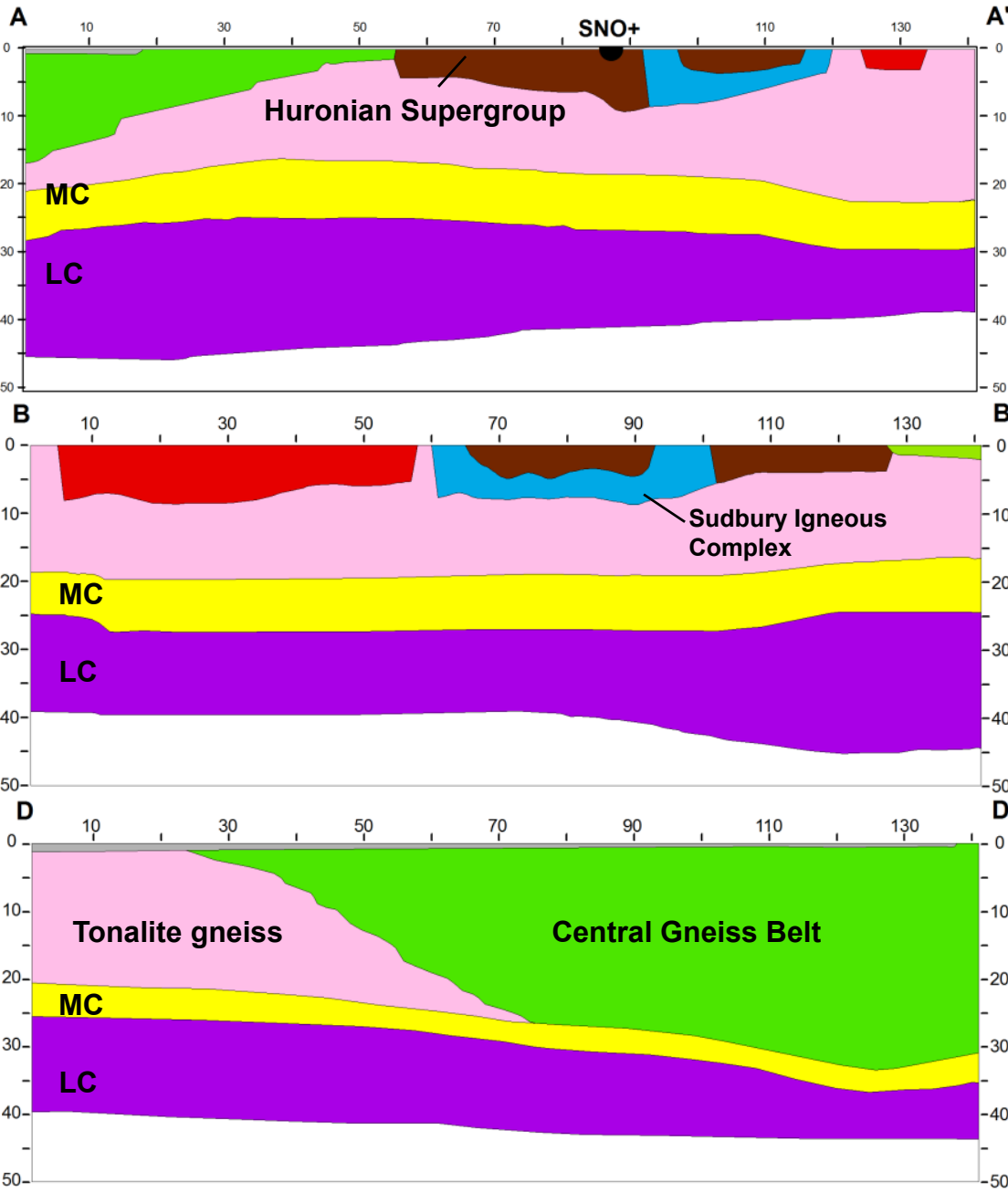
Output

Numerical **3D MODEL** made up of **VOXELS** of 1 km x 1 km x 100 m. Total Number of voxels $\sim 9 \times 10^7$.

	X	Y	Z	G
2996786	760000.00	5480000.00	-1300.00	2.00
2996787	770000.00	5480000.00	-1300.00	2.00
2996788	780000.00	5480000.00	-1300.00	2.00
2996789	790000.00	5480000.00	-1300.00	2.00
2996790	800000.00	5480000.00	-1300.00	2.00
2996791	810000.00	5480000.00	-1300.00	2.00
2996792	820000.00	5480000.00	-1300.00	2.00
2996793	830000.00	5480000.00	-1300.00	2.00
2996794	840000.00	5480000.00	-1300.00	2.00
2996795	850000.00	5480000.00	-1300.00	2.00
2996796	860000.00	5480000.00	-1300.00	2.00
2996797	870000.00	5480000.00	-1300.00	2.00
2996798	880000.00	5480000.00	-1300.00	2.00
2996799	890000.00	5480000.00	-1300.00	2.00



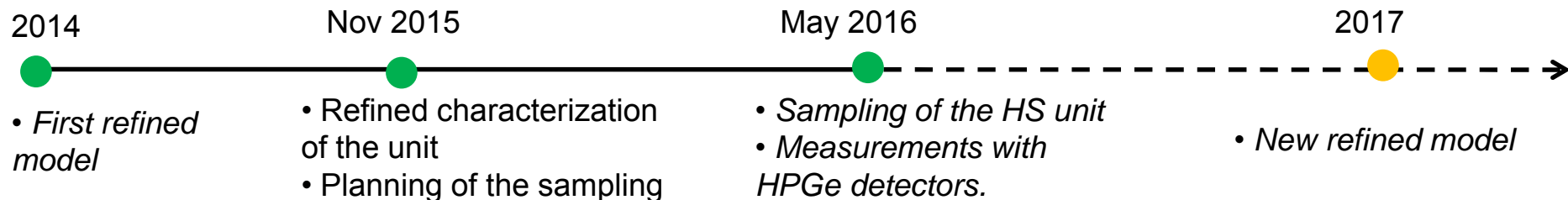
Virtual sections of the 3D model



Geoneutrino signal at SNO+ from the local crust

- After the refinement, the regional geoneutrino signal expected at SNO+ decreases from **18.9** $^{+3.5}_{-3.3}$ TNU (Huang et al. 2013) to **15.6** $^{+5.3}_{-3.4}$ TNU (Huang et al. 2014).
- The **Huronian Supergroup** is predicted to be the dominant source of the geoneutrino signal and the primary source of the large uncertainty.

Lithologic unit of UC	Vol. (%)	U (ppm)	Th (ppm)	S(U+Th) [TNU]
Tonalite/Tonalite gneiss (Wawa-Abitibi)	29.0	0.7 $^{+0.5}_{-0.3}$	3.1 $^{+2.3}_{-1.3}$	2.2 $^{+1.4}_{-0.9}$
Central Gneiss Belt (Grenville Province)	14.5	2.6 $^{+0.4}_{-0.4}$	5.1 $^{+6.0}_{-2.8}$	2.1 $^{+0.4}_{-0.3}$
(Meta)volcanic rocks (Abitibi sub-province)	1.4	0.4 $^{+0.4}_{-0.2}$	1.3 $^{+1.2}_{-0.6}$	0.02 $^{+0.01}_{-0.01}$
Paleozoic sediments (Great Lakes)	0.7	2.5 $^{+2.0}_{-1.1}$	4.4 $^{+1.6}_{-1.2}$	0.05 $^{+0.04}_{-0.02}$
Granite or granodiorite (Wawa-Abitibi)	1.0	2.9 $^{+1.6}_{-1.0}$	19.9 $^{+8.4}_{-6.0}$	0.5 $^{+0.2}_{-0.1}$
Huronian Supergroup, Sudbury Basin	1.3	4.2 $^{+2.9}_{-1.7}$	11.1 $^{+8.2}_{-4.8}$	7.3 $^{+5.0}_{-3.0}$
Sudbury Igneous Complex	0.1	2.3 $^{+0.2}_{-0.2}$	10.6 $^{+0.7}_{-0.7}$	0.8 $^{+0.1}_{-0.1}$
Middle Crust	15.0	0.8 $^{+0.5}_{-0.3}$	3.5 $^{+2.3}_{-1.6}$	1.2 $^{+0.7}_{-0.4}$
Lower Crust	37.0	0.2 $^{+0.2}_{-0.1}$	1.4 $^{+1.8}_{-0.7}$	0.7 $^{+0.6}_{-0.3}$



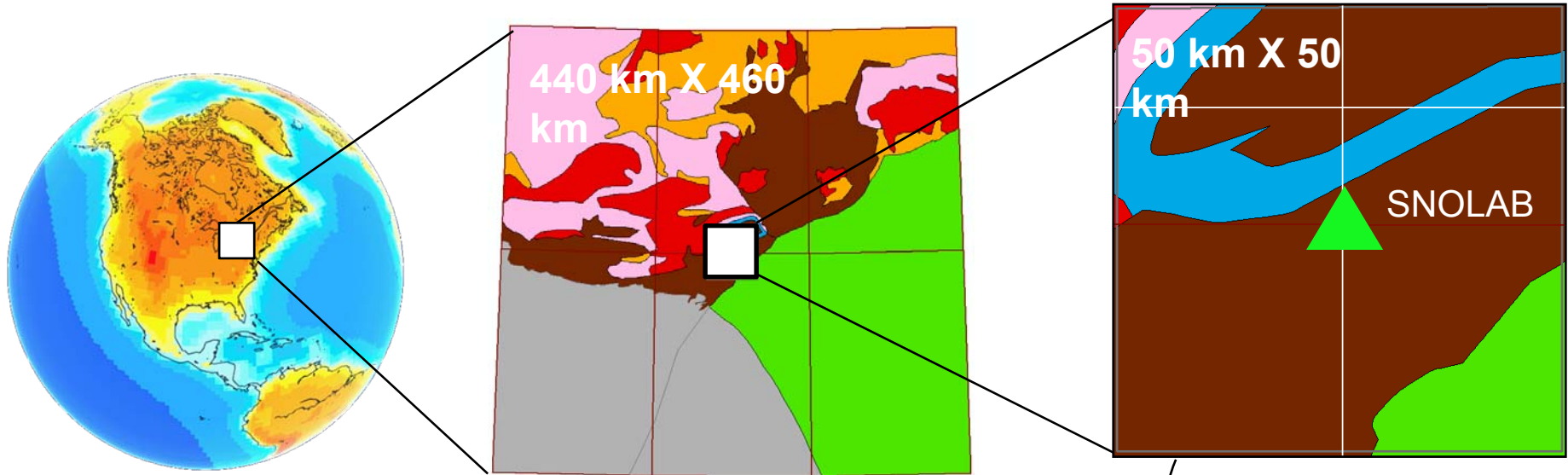
Focusing on close crust

Contribution to the crustal geoneutrino signal

48 %

26 %

26 %



92% of the signal of the HS-SB

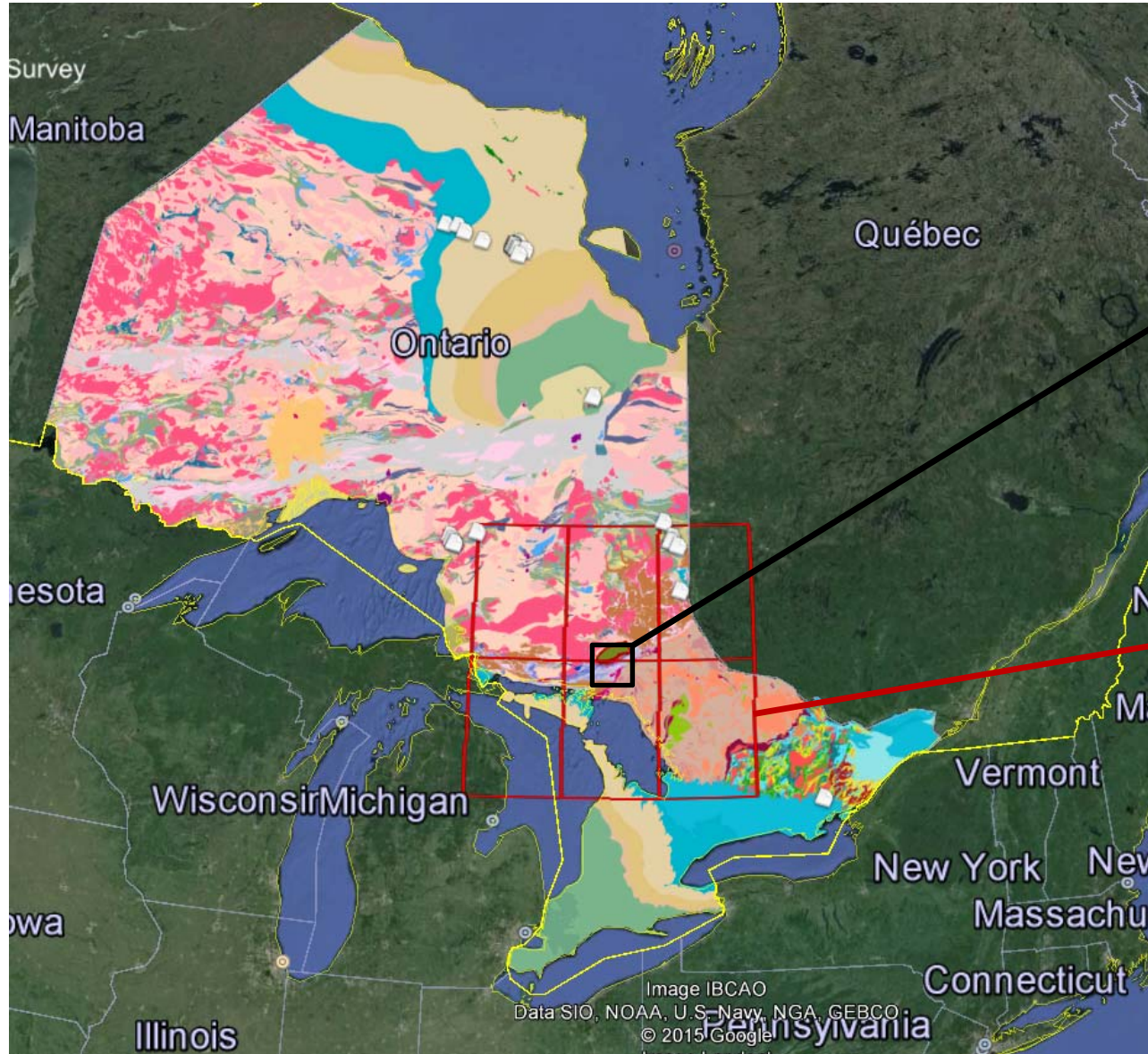
Global crustal model
Huang et al 2013

Local Crust (LOC)
Huang et al 2014

Close Crust (CLC)
New 3D geophysical
and geochemical model

Reference geological map

Bedrock Geology of Ontario map 1:250,000-scale. Ontario Geological Survey, Miscellaneous Release-Data 126, 2003



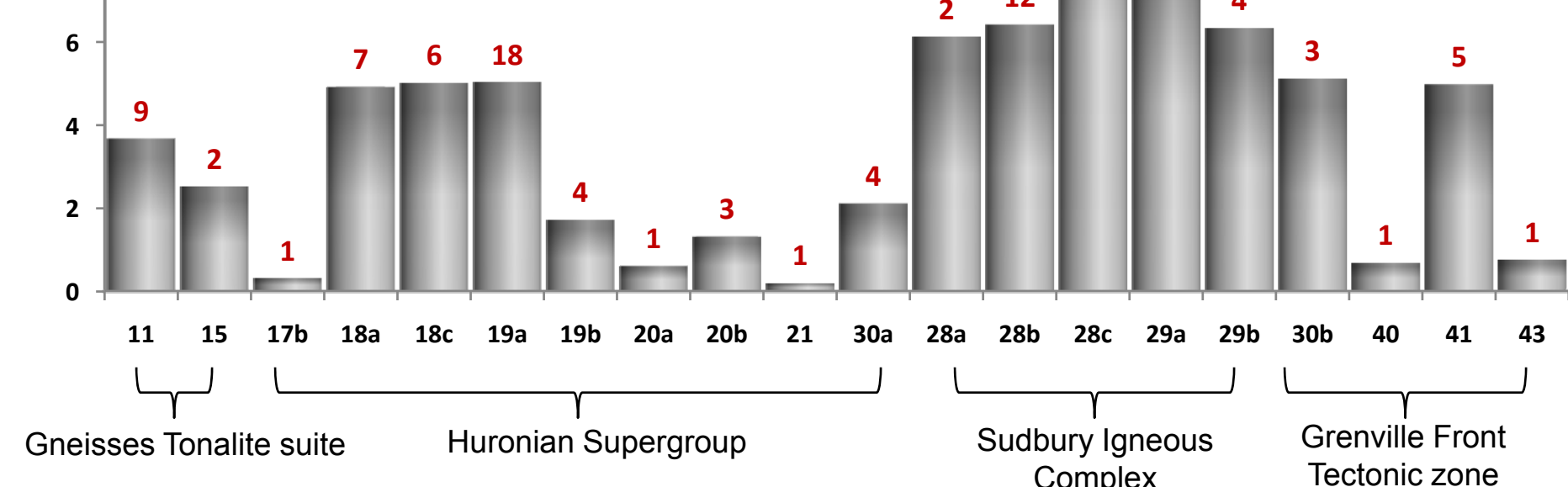
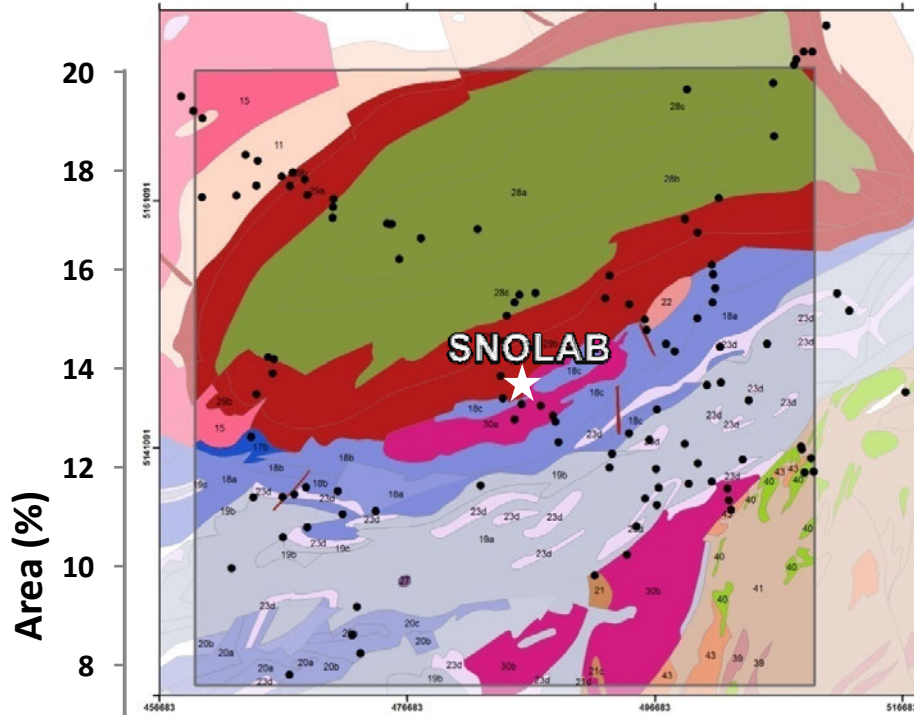
Close Crust
(CLC)
50 x 50 km

Local Crust
(LOC)
440 x 460 km

Rock sampling in the CLC

TOTAL SAMPLES = 112

- The sampling has been planned considering:
- exposure surface of reservoirs (A/S ~ 15 km²)
 - estimated volume
 - proximity to the detector
 - accessibility to the outcrops



Coming soon...

